# Robust Mosaicking of Stereo Digital Elevation Models from the Ames Stereo Pipeline

Taemin Kim[1], Zachary Moratto[1] and Ara V. Nefian[2]

1. NASA Ames Research Center, Moffett Field, CA, 94035
2. Carnegie Mellon University

**Abstract.** Robust estimation method is proposed to combine multiple observations and create consistent, accurate, dense Digital Elevation Models (DEMs) from lunar orbital imagery. The NASA Ames Intelligent Robotics Group (IRG) aims to produce higher-quality terrain reconstructions of the Moon from Apollo Metric Camera (AMC) data than is currently possible. In particular, IRG makes use of a stereo vision process, the Ames Stereo Pipeline (ASP), to automatically generate DEMs from consecutive AMC image pairs. However, the DEMs currently produced by the ASP often contain errors and inconsistencies due to image noise, shadows, etc. The proposed method addresses this problem by making use of multiple observations and by considering their goodness of fit to improve both the accuracy and robustness of the estimate. The stepwise regression method is applied to estimate the relaxed weight of each observation.

## 1. Introduction

Since 2007, the NASA Lunar Mapping and Modeling Project (LMMP) has been actively developing maps and tools to improve lunar exploration and mission planning [1]. One of the requirements for LMMP is to construct geo-registered DEMs from historic imagery. To meet this need, IRG has developed the Ames Stereo Pipeline (ASP), a collection of cartographic and stereogrammetric tools for automatically producing DEMs from images acquired with the Apollo Metric Camera (AMC) during Apollo 15-17 (**Figure 1**).

There are many applications of lunar maps, including outreach and education, mission planning, and lunar science. The maps and imagery that IRG released in 2009 for "Moon in Google Earth" have engendered great public interest in lunar exploration. The cartographic products that IRG is currently producing (DEMs, ortho-projected imagery, etc.) will be used to plan future missions, to assess landing sites, and to model geophysical processes. Consequently, by improving these maps, we directly benefit a wide community.

The NASA Ames Intelligent Robotics Group (IRG) currently uses a stereo vision process to automatically generate DEMs from image pairs [2]. However, two DEMs generated from different image pairs have different values for the same point due to noise, shadows, etc. in the images (**Figure 2**a). Consequently, IRG's current topographical

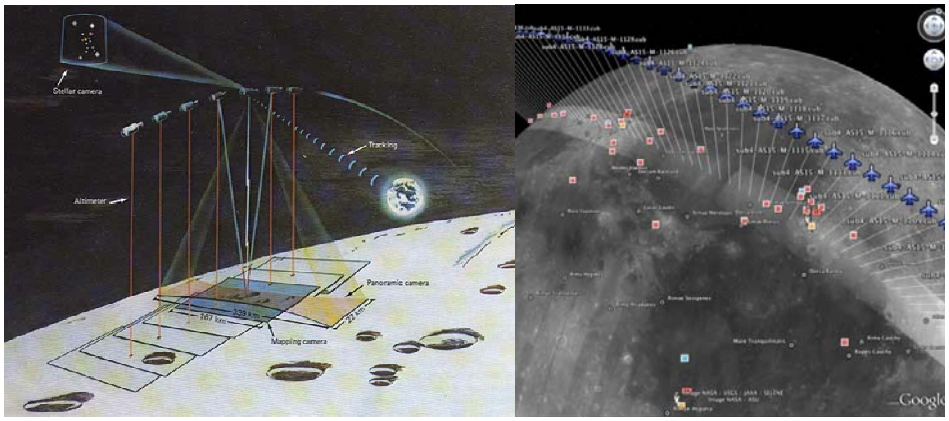


(a) The Mapping Cameras System (b) Apollo 15 Orbit 33

**Figure 1**: AMC Data System. (a) The AMC captures a series of pictures of the Moon's surface. (b) Satellite station positions for Apollo Orbit 33 visualized in Google Moon.

reconstruction of the Moon contains fairly substantial random errors (**Figure 2**b). It is important to construct consistent DEMs to estimate the photometric properties [3-5].

This paper will address this problem by finding robust elevation from multiple DEMs

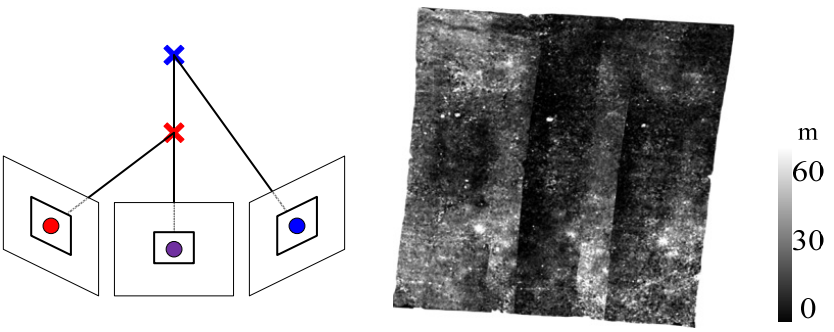


(a) Stereo Correspondences (b) DEM Errors

**Figure 2**: Stereo and Multiple View Correspondences. (a) Two stereo correspondences have different elevation values (two crosses). (b) DEMs created by stereo can have substantially large errors.

that minimize the weighted squared error of all associated DEM patches. The proposed method determines the unique 3D position by weighted averaging of all elevation values from stereo DEMs. The accuracy and robustness of DEMs produced by IRG will thus be improved by making use of multiple observations and by considering their goodness of fit. The reconstructed DEMs from lunar orbital imagery are presented. This paper tackles one of the challenging problems of planetary mapping from orbital imagery.

## 2. Ames Stereo Pipeline

The Ames Stereo Pipeline (ASP) is the stereogrammetric platform that was designed to process stereo imagery captured by NASA spacecraft and produce cartographic products since the majority of the AMC images have stereo companions [6]. The entire stereo correlation process, from an image pair to DEM, can be viewed as a multistage pipeline (**Figure 3**). At the first step, preprocessing includes the registration to align image pairs and filtering to enhance the images for better matching. Triangulation is used at the last step to generate a DEM from the correspondences.

### 2.1. Disparity Initialization

Stereo correlation, which is the process at the heart of ASP, computes pixel correspondences of the image pair (**Figure 4**). The map of these correspondences is called a *disparity map*. The best match is determined by applying a cost function that compares the two windows in the image pair. The normalized cross correlation is robust to slight lighting and contrast variation in between a pair of images [7]. For large images, this is computationally very expensive, so the correlation process is split into two stages. (1) The disparity map initialization step computes coarse correspondences using a multi-scale

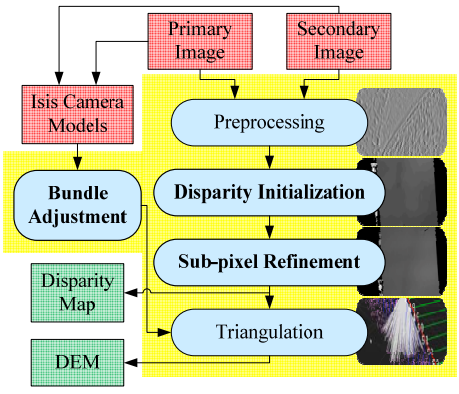


**Figure 3**: Dataflow of the Ames Stereo Pipeline. Preprocessing includes the registration and filtering of the image pair. A stereo correlator (disparity initialization and sub-pixel refinement) constructs the disparity map based on normalized cross correlation. DEMs are generated by a triangulation method in which corrected camera poses are used by bundle adjustment.

search that is highly optimized for speed (**Figure 4**c). (2) Correlation itself is carried out by sliding a small, square template window from the left image over the specified search region of the right image (**Figure 4**d-f).

Several optimizations are employed to accelerate disparity map initialization [8]: (1) a box-filter-like accumulator that reduces duplicate operations during correlation; (2) a coarse-to-fine multi-scale approach where disparities are estimated using low resolution images, and then successively refined at higher resolutions; and (3) partitioning of the disparity search space into rectangular sub-regions with similar values of disparity determined in the previous lower resolution level of the pyramid.

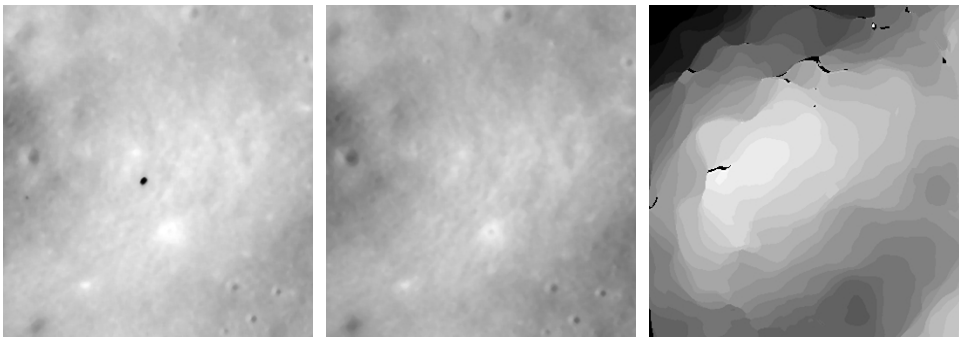

(a) Left Image (b) Right Image (c) Initialized Disparity Map

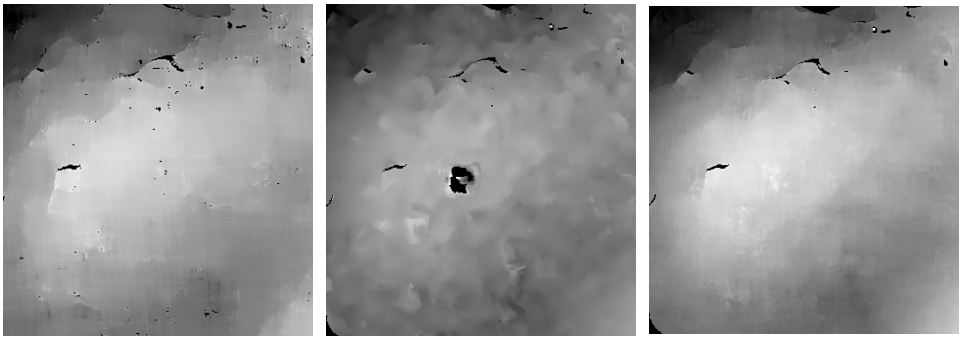

(d) Parabola Refined Map (e) Cauchy Refined Map (f) Bayesian Refined Map

**Figure 4**: Stereo Correlation. (a-b) An image pair. (c-f) Horizontal disparity maps. (c) The fast discrete correlator constructs the coarse disparity map. (d-f) Refined disparity maps from the initialized map. (f) Bayesian sub-pixel correlator generates a smoother map than the others.

## 2.2. Sub-pixel Refinement

Refining the initialized disparity map to sub-pixel accuracy is crucial and necessary for processing real-world data sets [9]. The Bayesian expectation maximization (EM) weighted affine adaptive window correlator was developed to produce high quality stereo matches that exhibit a high degree of immunity to image noise (**Figure 4**f). The Bayesian EM sub-pixel correlator also features a deformable template window that can be rotated, scaled, and translated as it zeros in on the correct match. This affine-adaptive window is essential for computing accurate matches on crater or canyon walls, and on other areas with significant perspective distortion due to foreshortening. A Bayesian model that treats the parameters as random variables was developed in an EM framework. This statistical model includes a Gaussian mixture component to model image noise that is the basis for the robustness of the algorithm. The resulting DEM is obtained by the triangulation method (**Figure 5**).

## 2.3. Bundle Adjustment

After stereo correlation is performed, Bundle Adjustment (BA) corrects the three-dimensional postures of cameras and the locations of the objects simultaneously to minimize the error between the estimated location of the objects and their actual location in the images. Camera position and orientation errors have a direct effect on the accuracy of DEMs produced by the ASP. If they are not corrected, these uncertainties will result in systematic errors in the overall position and slope of the DEMs (**Figure 6**a). BA ensures

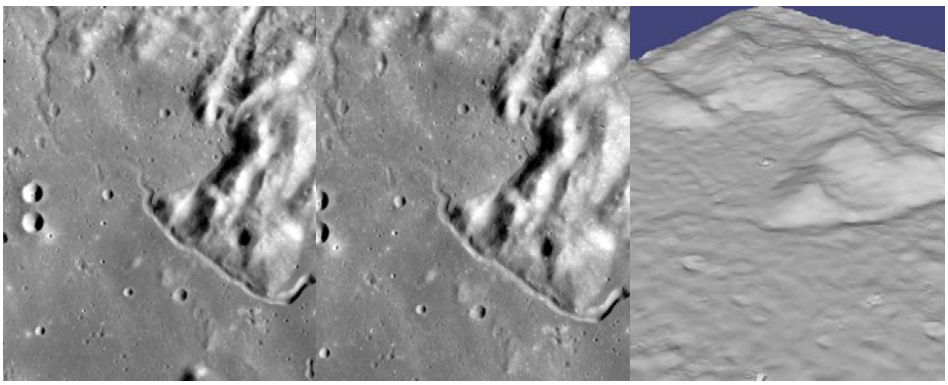

(a) Left Image (b) Right Image (c) Rendered DEM

**Figure 5**: Generation of DEM. (a) and (b) Apollo Metric Camera image pair of Apollo 15 site. (c) A DEM of Hadley Rille is rendered from an image pair.

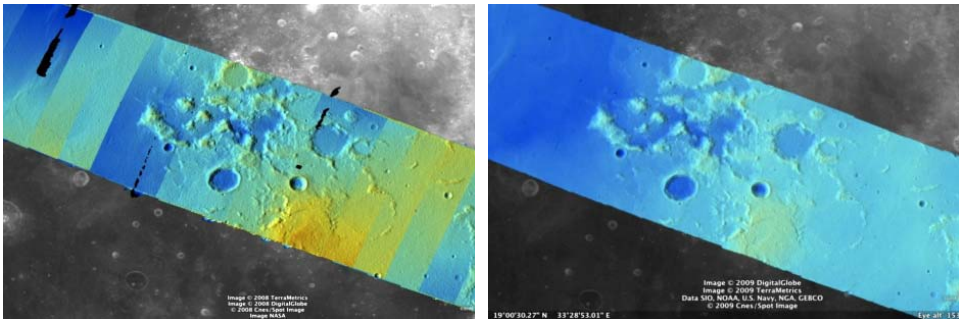

(a) Initial 3D Mesh (b) After Bundle Adjustment

**Figure 6**: Bundle Adjustment. Color-mapped, hill-shaded DEM mosaics from Apollo 15 Orbit 33 imagery illustrate the power of BA. (a) Prior to BA, large discontinuities exist between overlapping DEMs. (b) After BA, DEM alignment errors are minimized, and no longer visible.

that observations in multiple different images of a single ground feature are self-consistent (**Figure 6**b).

In BA the position and orientation of each camera station are determined jointly with the 3D position of a set of image tie-points points chosen in the overlapping regions between images. This optimization is carried out along with thousands (or more) of similar constraints involving many different features observed in other images. Tie-points are automatically extracted using the SURF robust feature extraction algorithm [10]. Outliers are rejected using the random sample consensus (RANSAC) method [11]. The BA in ASP determines the best camera parameters that minimize the reprojection error [12]. The optimization of the cost function uses the Levenberg-Marquardt algorithm [13].

## 3. Robust Estimation

Suppose a set of observations $P = \{x_k\}_{k=1}^{n}$ from a normal distribution with some of them are contaminated by outliers. Their Boolean membership to inliers is represented by an indicator vector $\mathbf{w} = [w_k] \in \{0,1\}^n$:

$$w_k = \begin{cases} 0 \text{ if } x_k \text{ is outlier} \\ 1 \text{ otherwise.} \end{cases} \quad (1)$$

Let $w$ be the total number of inliers:

$$w = \sum_{i=1}^{n} w_k. \tag{2}$$

The membership measure supporting the normality is defined to minimize its square error and to maximize the number of inliers. The mean of the inliers is written by

$$\bar{x} = \frac{1}{w}\sum_{i=1}^{n} w_k x_k \ . \tag{3}$$

The squared error is written by

$$\begin{aligned} SSE &= \sum_{k=1}^{n} w_k (x_k - \bar{x})^2 \\ &= \frac{\sum_{k=1}^{n} w_k \sum_{k=1}^{n} w_k x_k^2 - \left(\sum_{k=1}^{n} w_k x_k\right)^2}{\sum_{k=1}^{n} w_k}, \end{aligned} \tag{4}$$

An objective function which minimizes $s^2$ and maximizes $w$ simultaneously is hard to define. Even if it is defined, computing the optimum **w** is NP-hard.

The Boolean membership vector is relaxed to be a real value in [0,1] to convert the combinatorial optimization problem into a tractable nonlinear optimization problem [14]. The membership matrix reflects the likelihood of the inliers. Let us redefine $\mathbf{w} = [w_i] \in [0,1]^n$, where $w_i$ is the membership of point $x_i$ to inliers. Then the equations from (3) to (7) are still valid. From the expected value of $SSE$,

$$E(SSE) = \left(w - \frac{1}{w}\sum_{k=1}^{n} w_k^2\right)\sigma^2, \tag{5}$$

The mean squared error is defined by

$$MSE = \frac{wSSE}{w^2 - \sum_{k=1}^{n} w_k^2} = \frac{\sum_{k=1}^{n} w_k \sum_{k=1}^{n} w_k x_k^2 - \left(\sum_{k=1}^{n} w_k x_k\right)^2}{\left(\sum_{k=1}^{n} w_k\right)^2 - \sum_{k=1}^{n} w_k^2}, \tag{6}$$

The squared error of each point is defined by

$$\frac{\partial SSE}{\partial w_i} = (x_i - \bar{x})^2, \tag{7}$$

The statistic to test statistical significance for $x_i$ follows the *F* distribution:

$$s_i = \frac{(x_i - \bar{x})^2}{v_i} \Bigg/ \frac{\sum_{k=1}^{n} w_k x_k^2 - \bar{x}^2}{v} \sim F_{v_i, v}, \tag{8}$$

where $v_i$ and $v$ are the degrees of freedom such that

$$v_i = 1 - \frac{w_i}{w} \text{ and } v = w - \frac{1}{w}\sum_{k=1}^{n} w_k^2 \tag{9}$$

The updating principle is to increase the weight of a observation if its *p*-value of the statistic is smaller than the significance level or to decrease the weight. Similar with the gradient descent method, the update rule is implemented by

$$\Delta w_i = \eta \left\{ 1 - F_{v_i, v}^{-1}(s_i) - \alpha \right\}, \tag{10}$$

where $\alpha$ and $\eta$ are significance level and learning rate.

## 4. Experimental Results

The NASA Exploration Systems Mission Directorate (ESMD) has been charged with producing cartographic products via LMMP for use by mission planners and scientists in NASA's Constellation program. As part of the LMMP, we have produced 70 preliminary DEMs and ortho-images derived from Apollo 15 Metric Camera (AMC) orbit 33 imagery using the ASP. The DEM Mosaic program is implemented based on the NASA Vision Workbench (VW). The NASA VW is a general purpose image processing and computer

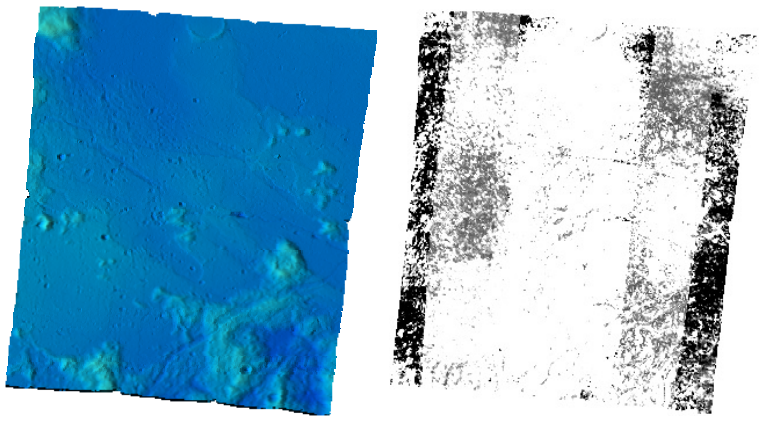

(a) Robust DEM Mosaic (b) Weight Image

**Figure 7**: DEM Mosaic and its weight.

vision library developed by the IRG at the NASA Ames Research Center.

The unified DEM mosaics are constructed with the stereo DEMs. The significance level $\alpha$ was set to be 0.3 and the typical learning rate $\eta$ is 0.01. **Figure 7**a shows a DEM mosaic image constructed from its adjacent stereo DEMs which has large variances between DEMs as shown in **Figure 2**b. As you can see in the figure, the unified DEM mosaic provides the seamless elevation map. **Figure 7**b shows the estimated weight for the current DEM as we can expected that the central part of the DEM has large confidence.

## 5. Conclusion

The robust estimation method was proposed to determine the unique elevation from multiple digital elevation models generated by the Ames Stereo Pipeline. Introducing the relaxed membership of each observation to be an inlier, the stepwise regression method is applied to estimate the relaxed weight of the observation. The proposed method addresses this problem by making use of multiple observations and by considering their goodness of fit to improve both the accuracy and robustness of the estimate. A gradient descent method was used to optimized the weight because it is hard to define the objective function in a closed form. The residual analysis will be desirable to provide a quantitative measure of the proposed method. The parametric representation of surface model will be valuable to enhance the recovery resolution and robustness of the algorithm.

## 6. Acknowledgement

This research was supported by an appointment to the NASA Postdoctoral Program at the Ames Research Center, administered by Oak Ridge Associated Universities through a contract with NASA.

## 7. References

1. Noble, S.K., et al., *The Lunar Mapping and Modeling Project.* LPI Contributions, 2009. **1515**: pp. 48.
2. Broxton, M., et al., *3D Lunar Terrain Reconstruction from Apollo Images.* Advances in Visual Computing, 2009. pp. 710-719.
3. Kim, T., A.V. Nefian, and M.J. Broxton, *Photometric recovery of Apollo metric imagery with Lunar-Lambertian reflectance.* Electronics Letters. **46**: pp. 631.
4. Kim, T., A. Nefian, and M. Broxton, *Photometric Recovery of Ortho-Images Derived from Apollo 15 Metric Camera Imagery.* Advances in Visual Computing, 2009. pp. 700-709.
5. Nefian, A.V., et al. *Towards Albedo Reconstruction from Apollo Metric Camera Imagery*: pp. 1555.
6. Broxton, M.J., et al., *The Ames Stereo Pipeline: NASA's Open Source Automated Stereogrammetry Software*. 2009, NASA Ames Research Center.

7. Menard, C., *Robust Stereo and Adaptive Matching in Correlation Scale-Space*. 1997, Institute of Automation, Vienna Institute of Technology.
8. Sun, C., *Fast stereo matching using rectangular subregioning and 3D maximum-surface techniques.* International Journal of Computer Vision, 2002. **47**(1): pp. 99-117.
9. Nefian, A., et al. *A Bayesian Formulation for Subpixel Refinement in Stereo Orbital Imagery*. in *International Conference on Image Processing*. 2009. Cairo, Egypt.
10. Bay, H., et al., *Speeded-up robust features (SURF).* Computer Vision and Image Understanding, 2008. **110**(3): pp. 346-359.
11. Fischler, M.A. and R.C. Bolles, *Random sample consensus: A paradigm for model fitting with applications to image analysis and automated cartography.* Commun. Assoc. Comp. Mach,, 1981. **24**(6): pp. 381-395.
12. Triggs, B., et al., *Bundle adjustment - a modern synthesis.* Lecture Notes in Computer Science, 1999. pp. 298-372.
13. Hartley, R. and A. Zisserman, *Multiple view geometry in computer vision*. 2003: Cambridge University Press.
14. Kim, T., J. Woo, and I.S. Kweon. *Probabilistic matching of lines for their homography*. 2009: pp. 3453-3456.